

Paramagnetic Cobalt(II) as a Probe for Kinetic and NMR Relaxation Studies of Phosphate Binding and the Catalytic Mechanism of *Streptomyces* Dinuclear Aminopeptidase

Michael N. Harris, Craig M. Bertolucci, and Li-June Ming*

Department of Chemistry and Institute for Biomolecular Science, University of South Florida, 4202 Fowler Avenue, Tampa, Florida 33620-5250

Received March 11, 2002

Phosphate was proposed to be a bridging ligand in the structure 1xjo.pdb of *Streptomyces* dizinc aminopeptidase (sAP), which prompted further studies of phosphate binding to this enzyme. Phosphate inhibits sAP and its Co²⁺-substituted derivatives in a noncompetitive manner from pH 6.0 to 9.0, with strongest inhibition observed at lower pHs ($K_i = 0.6, 8.2,$ and 9.1 mM for ZnZn-, CoCo-, and CoZn-sAP, respectively, at pH 6.0), which indicates that phosphate does not compete with substrate binding to the dinuclear active site and that monobasic phosphate has a higher binding affinity. The inhibition K_i -pH profiles for phosphate inhibition of both the native and the Co²⁺-substituted derivatives reveal a similar pK_a around 7.0, reflecting that phosphate binding is not affected by the metal centers of different Lewis acidities. Modification of ZnZn- and CoCo-sAP with the arginine-specific reagent phenylglyoxal reveals a significant weakening in phosphate and substrate binding by showing approximately a 10-fold increase in the dissociation constant K_i for phosphate binding and ~ 4 – 8 -fold increase in K_m . The catalysis is also influenced by the modification as reflected by a significant decrease in k_{cat} in both cases. Furthermore, phosphate and the transition-state inhibitor 1-aminobutyl phosphonate can protect arginine from the modification, strongly suggesting that Arg202 near the active site is involved in phosphate binding and in stabilizing the transition state. The effect on ³¹P NMR relaxation of phosphate caused by the paramagnetic metal center in Co²⁺-substituted derivatives of sAP has been measured, which reveals that only one phosphate is bound to sAP with the Co²⁺-³¹P distance in the range of 4.1–4.3 Å. The ¹H NMR relaxation of the bulk water signal in the CoCo-sAP sample remains unchanged in the presence of phosphate, further indicating that phosphate may not bind to the active-site metals to displace any metal-bound water/hydroxide. These results strongly support that the phosphate binding site is Arg202 and that this residue plays an important role in the action of sAP.

Introduction

Aminopeptidases (APs) catalyze the hydrolysis of protein and peptide substrates from the N-terminus and are ubiquitously found in all three domains, the Bacteria, the Archaea, and the Eukarya.^{1–3} Several biological processes require aminopeptidases to act properly, such as hormone-level regulation, protein maturation, and terminal degradation of proteins.^{4–7} The aminopeptidases from bovine lens (bLAP),^{8–13}

Aeromonas proteolytica (aAP),^{14,15} and *Streptomyces griseus* (sAP)^{16,17} have been demonstrated by means of crystal-

* Corresponding author. Tel: 813-974-2220. Fax: 813-974-1733. E-mail: Ming@chuma.cas.usf.edu.

- (1) Taylor, A. *FASEB J.* **1993**, *7*, 290–298.
- (2) Taylor, A. *Trends Biochem. Sci.* **1993**, *18*, 167–172.
- (3) Taylor, A.; Brown, M. J.; Daims, M. A.; Cohen, J. *Invest. Ophthalmol. Vis. Sci.* **1983**, *24*, 1172–1181.
- (4) Taylor, A.; Daims, M. A.; Lee, J.; Surgenor, T. *Curr. Eye Res.* **1982**, *2*, 47–56.

- (5) Frost, P.; Greig, R. *The Role of Cellular Proteases and Inhibitors in Invasion and Metastasis*; Kluwer: New York, 1990.
- (6) Kempt, D. J. *Met. Enzymol.* **1994**, *241*, 334–370.
- (7) Umezawa, H. *Recent Results Cancer Res.* **1980**, *75*, 115–125.
- (8) Burley, S. K.; David, P. R.; Sweet, R. M.; Taylor, A.; Lipscomb, W. N. *J. Mol. Biol.* **1990**, *224*, 113–140.
- (9) Burley, S. K.; David, P. R.; Taylor, A.; Lipscomb, W. N. *Proc. Natl. Acad. Sci. U.S.A.* **1990**, *87*, 6878–6882.
- (10) Burley, S. K.; David, P. R.; Lipscomb, W. N. *Proc. Natl. Acad. Sci. U.S.A.* **1991**, *88*, 6916–6920.
- (11) Strater, N.; Lipscomb, W. N. *Biochemistry* **1995**, *34*, 9200–9210.
- (12) Strater, N.; Lipscomb, W. N. *Biochemistry* **1995**, *34*, 14792–14800.
- (13) Burley, S. K.; David, P. R.; Sweet, R. M.; Taylor, A.; Lipscomb, W. N. *J. Mol. Biol.* **1992**, *224*, 113–140.
- (14) Chevrier, B.; Schalk, C.; D'Orchymont, H.; Rondeau, J.-M.; Moras, D.; Tarnus, C. *Structure* **1994**, *2*, 283–291.
- (15) Chevrier, B.; D'Orchymont, H.; Schalk, C.; Tarnus, C.; Moras, D. *Eur. J. Biochem.* **1996**, *237*, 393–398.

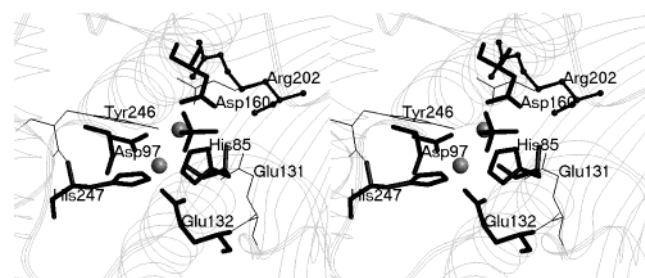


Figure 1. Stereoview of the dizinc active site in sAP with a nonprotein ligand, suggested as phosphate (Protein Data Bank code 1xjo).¹⁶ This phosphate is replaced with a bridging hydroxide in a later structure (1cp7) with Zn–O distances of 2.16 and 2.28 Å and Zn–Zn distance of 3.60 Å,¹⁷ comparable to those in the 1xjo structure (1.99, 2.30, and 3.64 Å, respectively). The structure 1xjo does not reveal the loop region 196–202, which is shown in a later structure (1qq9). The Arg202 side chain in this figure has been added by the use of the Swiss PdbViewer Version 3.5 program on the basis of the structure 1xjo. There are several possible low-energy conformers for this Arg side chain as it is exposed to the solvent. The two conformers shown here can bring the guanidinium center near the metal centers in the range of ~6.5–7.5 Å (ball-and-stick conformer) or ~5–5.5 Å (thin-line conformer). Binding of the phosphate to the guanidinium group of the former conformer can afford metal–³¹P distances of ~4.1–4.5 Å. In the latter case, H-bonding interactions can be expected between the side chain of Arg202 and a *gem*-diolate-like transition state structure in the active site, suggesting the significance of this residue in sAP action.

lography to contain a unique dizinc active site with the two zinc ions roughly 2.8–3.6 Å apart, bridged by an aspartic acid side chain and a water or hydroxide.

S. griseus aminopeptidase is an extracellular enzyme with a preference for large hydrophobic amino terminus residues^{18,19} and is activated by calcium.²⁰ The structure of sAP has recently been resolved by means of X-ray crystallography.^{16,17} The solvent-accessible active site of sAP with its coordinating ligands and some neighboring residues are shown in Figure 1. In the first published structure,¹⁶ the two zinc ions are found to be 3.6 Å apart and are bridged by Asp97 and a nonprotein ligand that is suggested to be a monobasic phosphate ion. This bridging phosphate is replaced by a bridging water or hydroxide in aAP,¹⁴ bIAP,⁹ and another structure of sAP.¹⁷ The binding nature of phosphate in the crystal structure of sAP is similar to that of the phospho moiety of transition-state analogues upon binding to aAP and bIAP with one of the phosphoryl oxygens bridging the two zinc ions.^{11,12,15}

The similar binding nature of the phospho-containing inhibitors toward these dinuclear APs (i.e., binding to and bridging the metal ions) suggests that phosphate may behave as a simplest analogue of the transition state *gem*-diolate moiety of peptide substrates and thus may compete with substrate binding to the active-site metal. However, non-competitive inhibition was observed in a recent kinetic study

of phosphate inhibition toward sAP from pH 5.8 to 9.0,²¹ suggesting that phosphate may not bind to the active metal ions. This inconsistency has inspired a more detailed investigation of the phosphate binding nature of sAP. We report herein nuclear magnetic resonance (NMR) relaxation and kinetic studies of phosphate binding to native ZnZn-sAP and its Co²⁺-substituted derivatives. The distance between the active site metal ions and the phosphate binding site has been determined by means of ³¹P NMR relaxation. Moreover, chemical modification has provided insight into phosphate binding and the mechanistic role of a specific arginine near the active site.

Experimental Procedures

Materials and Reagents. The crude enzyme mixture Pronase, the buffers MES (2-morpholinoethanesulfonic acid) and HEPES (*N*-(2-hydroxyethyl)piperazine-*N'*-2-ethanesulfonic acid), NaH₂PO₄, EDTA (ethylenediaminetetraacetic acid), and 1,10-phenanthroline, (diethylamino)ethyl (DEAE)-Sephacel, Sephadex G-50, phenylglyoxal monohydrate, and the substrate l-leucine-*p*-nitroanilide (Leu-*p*NA) were purchased from Sigma-Aldrich Chemical Co. (St. Louis, MO). Zinc(II) and cobalt(II) stock solutions were prepared from atomic absorption standard (>99.99%) purchased from Fisher Scientific (Pittsburgh, PA) or from corresponding metal salts (>99.95%) and standardized with standard EDTA. All solutions were prepared from deionized water of >18 MΩ from a MilliQ system (Millipore, Bedford, MA). The glassware and plastic ware were treated with EDTA and rinsed with deionized water prior to use.

Enzyme Preparation and Kinetics. The enzyme sAP and its apo form were prepared according to the literature procedures.^{18,19} The enzyme concentration was determined according to the absorption value $E^{1\%}_{280} = 15$.¹⁸ The derivative CoE-sAP (E is an empty site) was prepared by adding 1 equiv of Co²⁺ to apo-sAP and characterized with electronic and NMR spectroscopies according to the literature.^{22,23} Once CoE-sAP is formed, 1 equiv of Zn²⁺ is added slowly until complete formation of CoZn-sAP and verified by the emergence of a new ¹H NMR spectrum.

Kinetic measurements were performed on a Varian Cary 3E spectrophotometer using the substrate Leu-*p*NA from pH 6.0 to 8.0. Assays were performed in 50 mM buffer, 60 mM NaNO₃ for ionic strength, and 0.1 mM metal ions at 30 °C. The rate of Leu-*p*NA hydrolysis by CoZn-sAP without excess metal ions was constant throughout the assay, indicating that the active site remained intact during the entire assay time. The initial rate of hydrolysis of the substrate was observed by monitoring the release of the chromophore *p*NA at 405 nm ($\epsilon = 10\,500\text{ M}^{-1}\text{ cm}^{-1}$ which is constant in the pH range). The kinetic parameters k_{cat} and K_m were obtained by nonlinear fitting of the data to the hyperbolic Michaelis–Menten equation, i.e., $\text{rate} = k_{\text{cat}}[E_0][S]/(K_m + [S])$, with $[E_0]$ the enzyme concentration ranging between 1.0 and 4.0 nM and $[S]$ the substrate concentration at 0.25–10 mM. The catalytic inhibition constant K_i for noncompetitive inhibition pattern is obtained by fitting the apparent rate V_{app} with respect to the inhibitor concentration $[I]$ to the equation $V_{\text{app}} = V/(1 + [I]/K_i)$, or by the Dixon plot.²⁴

(16) Greenblatt, H. M.; Almog, O.; Maras, B.; Spungin-Bialik, A.; Barra, D.; Blumberg, S.; Shoham, G. *J. Mol. Biol.* **1997**, *265*, 620–636.

(17) Gilboa, R.; Greenblatt, H. M.; Perach, M.; Spungin-Bialik, A.; Lessel, U.; Wohlfahrt, G.; Schomburg, D.; Blumberg, S.; Shoham, G. *Acta Cryst. D* **2000**, *56*, 551–558.

(18) Spungin, A.; Blumberg, S. *Eur. J. Biochem.* **1989**, *183*, 471–477.

(19) Ben-Meir, D.; Spungin, A.; Ashkenazi, R.; Blumberg, S. *Eur. J. Biochem.* **1993**, *212*, 107–112.

(20) Papir, G.; Spungin-Bialik, A.; Ben-Meir, D.; Fudim, E.; Gilboa, R.; Greenblatt, H. M.; Shoham, G.; Lessel, U.; Schomburg, D.; Ashkenazi, R.; Blumberg, S. *Eur. J. Biochem.* **1998**, *258*, 313–319.

(21) Harris, M. N.; Ming, L.-J. *FEBS Lett.* **1999**, *455*, 321–324.

(22) Lin, L.-Y.; Park, H.-I.; Ming, L.-J. *J. Biol. Inorg. Chem.* **1997**, *2*, 744–749.

(23) Lin, L.-Y. M.S. Thesis, University of South Florida, 1996.

(24) Dixon, N. E.; Blakely, R. L.; Zerner, B. *Can. J. Biochem.* **1980**, *58*, 481–488.

Modification of Arginine. Chemical modification of arginine residues in sAP with phenylglyoxal was performed according to the literature procedures in both 0.1 M bicarbonate and borate solutions.²⁵ Borate was found to assist the modification reaction slightly better than carbonate and thus was used in this study. An enzyme solution of 1.5 μ M was incubated in 2.0 mM phenylglyoxal at pH 8.5, followed by thorough dialysis against buffer at pH 5.5 to remove the excess phenylglyoxal and to ensure stabilization of the modified form. Aliquots of the modified enzyme were diluted further and subjected to kinetic measurements.

NMR Spectra and Relaxation. The isotropically shifted ^1H NMR spectra of the metal-substituted derivatives (~ 1 mM) were obtained at 298 K on a Bruker AMX360 spectrometer using a WEFT sequence to suppress water and the diamagnetic protein signals. Spectra of the samples in 10% D_2O consisted of about 10 000 scans with 8 K data points. Chemical shifts were measured from the bulk water signal assumed to be at 4.65 ppm downfield from TMS. A 10–30 Hz additional line broadening was introduced by exponential multiplication of the FID to improve the signal-to-noise ratio. ^{31}P NMR T_1 relaxation at 145.73 MHz on the Bruker AMX360 was measured with the inversion–recovery method, and the values were obtained with a nonlinear three-parameter least-squares fitting program. An error of less than 10% in the T_1 values is estimated on the basis of the fitting and repeating measurements. The ^{31}P NMR T_1 values of phosphate in the presence of the paramagnetic protein CoZn- and CoCo-sAP and the diamagnetic ZnZn-sAP were measured at protein concentrations of ~ 1 mM and phosphate concentrations in the range of 10–230 mM.

Results and Discussion

Preparation of Co^{2+} -Substituted Derivatives. To obtain a clear picture about phosphate binding to sAP, paramagnetic Co^{2+} derivatives of sAP are prepared and the paramagnetic contribution to ^{31}P NMR relaxation is measured. The formation of different Co^{2+} -substituted derivatives must be confirmed for this purpose. It has been previously demonstrated that 1 equiv of Co^{2+} binds selectively to apo sAP to form a mono- Co^{2+} -substituted derivative of sAP, dubbed CoE-sAP with an empty second site “E”.^{22,23} The addition of 1 equiv of Co^{2+} and Zn^{2+} to CoE-sAP results in the formation of the derivatives CoCo-sAP²² and CoZn-sAP, respectively, which show characteristic hyperfine-shifted ^1H NMR spectra different from each other and from that of CoE-sAP (Figure 2).²² The different NMR spectra confirm the formation of the different derivatives. Particularly, the NMR spectra clearly show that Zn^{2+} is bound to the empty site to afford the desired CoZn-sAP derivative with only one paramagnetic center, but Zn^{2+} does not replace the Co^{2+} in CoE-sAP to generate a mixture of different derivatives. Hyperfine-shifted solvent exchangeable signals attributed to the ring-NH proton of the His residues coordinated to Co^{2+} can be recognized which disappear in D_2O buffers^{26,27} (asterisked signals in Figure 2), i.e., one signal in CoE- and CoZn-sAP and two signals in CoCo-sAP. This is consistent

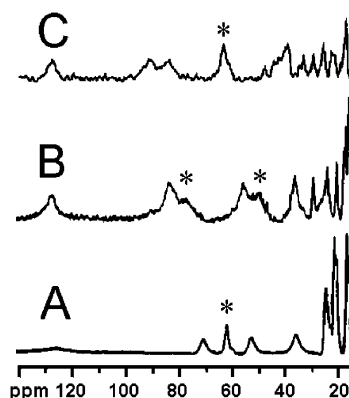


Figure 2. Hyperfine-shifted ^1H NMR “fingerprints” of the Co^{2+} -substituted derivatives of sAP (360 MHz, 298 K, pH 6.0): (A) CoE-sAP; (B) CoCo-sAP; (C) CoZn-sAP. The solvent exchangeable signals are labeled with asterisks, which disappear when the proteins are dissolved in D_2O buffer and are assigned to the ring NH protons of the coordinated His in the Co^{2+} site. The different spectral features confirm the formation of the derivatives.

with the observation in the crystal structure where one His is found in each of the metal binding sites (Figure 1).

The addition of Zn^{2+} to CoE-sAP results in the appearance of two far-shifted signals at 83.5 and 91.0 ppm with concomitant decrease in intensity of the two signals at 53.5 and 71.5 ppm. These two signals disappear completely upon addition of 1 equiv of Zn^{2+} , whereas the signals at 127.7 and 37.6 ppm and the solvent-exchangeable ring-NH signal of a coordinated His at 62.8 ppm are little affected (Figure 2C). As the ring-CH protons of a N_ϵ -coordinated His residue are extremely broad and in most cases beyond detection, the non-solvent-exchangeable hyperfine-shifted ^1H NMR signals are most possibly attributable to the C_βH_2 and/or $\text{C}_\gamma\text{H}_2$ protons of a coordinated Asp and/or Glu, respectively.^{26,27} The highly affected signals at 53.5 and 71.5 ppm upon Zn^{2+} binding can be reasonably assigned to the C_βH_2 protons of Asp97 (Figure 1). This Asp is originally coordinated to Co^{2+} in CoE-sAP and becomes a bridging ligand upon Zn^{2+} binding to the empty site, thus is expected to be affected the most. Whether the unaffected signals are due to the C_βH_2 of Asp160 or $\text{C}_\gamma\text{H}_2$ of Glu132 cannot be determined to definitely assign the Co^{2+} binding site in CoE-sAP and CoZn-sAP. This derivative with only one paramagnetic Co^{2+} center allows unambiguous results to be obtained in the relaxation study discussed later. Zn^{2+} does not selectively bind to one site of sAP to give “ZnE-sAP”;²² thus, the derivative ZnCo-sAP cannot be prepared.

Phosphate Inhibition of sAP and Its Metal Derivatives. Phosphate inhibition of CoCo- and CoZn-sAP toward the hydrolysis of Leu-*p*NA has been examined in a pH range of 6.0–9.0. Phosphate was found to be a noncompetitive inhibitor throughout the pH range and exhibited higher degree of inhibition at lower pH, showing an inhibition constant $K_i = 9.1 \pm 0.4$ mM for CoCo-sAP and 8.2 ± 0.3 mM for CoZn-sAP at pH 6.0 (Figure 3). Plot of K_i values against pH reveals $\text{p}K_a$ values of 7.10 ± 0.08 and 6.91 ± 0.05 associated with phosphate binding to CoCo-sAP and CoZn-sAP, respectively (insets, Figure 3). In addition, the activity approaches zero when phosphate concentration is high (data not shown). These results indicate that phosphate

(25) Takahashi, K. *J. Biol. Chem.* **1968**, *243*, 6171–6179.

(26) Bertini, I.; Luchinat, C. *NMR of Paramagnetic Molecules in Biological Systems*; Benjamin/Cummings: Menlo Park, CA, 1986.

(27) Ming, L.-J. In *Physical Methods in Bioinorganic Chemistry, Spectroscopy and Magnetism*; Que, L., Jr., Ed.; University Science Books: Mill Valley, CA, 2000.

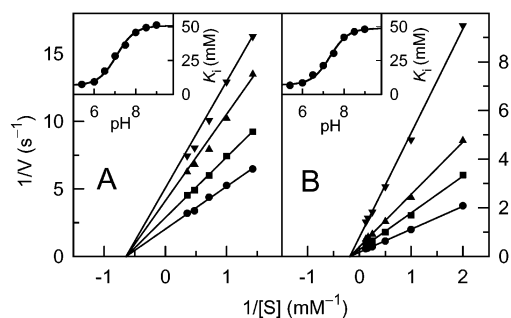


Figure 3. Plot of inverse rate V^{-1} versus inverse substrate concentration $[S]^{-1}$ at pH 6.0 for phosphate inhibition of (A) CoCo-sAP and (B) CoZn-sAP. Phosphate concentration are 0.0 (●), 4.0 (■), 15 (▲), and 30 (▼) mM in (A) and 0.0 (●), 5.0 (■), 10 (▲), and 20 (▼) mM in (B). The noncompetitive inhibition pattern is determined on the basis of the k_{cat} and K_m values obtained from nonlinear fitting of the data to the Michaelis–Menten equation, in which the K_m values are not varied with inhibitor concentration. The inhibition constants are found to be 9.1, 8.2, and 0.80 mM for phosphate binding to CoCo-, CoZn-, and ZnZn-sAP,²¹ respectively, under these conditions. The insets show the pH dependence of phosphate inhibition constants of CoZn-sAP and CoCo-sAP, fitted to a one-deprotonation process to give $\text{p}K_a$ values of 6.91 and 7.10 (and 7.1 for ZnZn-sAP²¹), respectively.

serves as a “pure noncompetitive inhibitor” and is not competing with the substrate in binding to the same site,²⁸ presumably the metal ions in the active site. In a pure noncompetitive inhibition, the inhibitor can bind to both the enzyme (E) and the enzyme–substrate complex (ES) to afford the enzyme–inhibitor complex (EI) and the enzyme–substrate–inhibitor ternary complex (ESI), respectively, with the same inhibition constant. However, the ESI complex is inert which does not yield products.²⁸ Phosphate was found to also inhibit native sAP (ZnZn-sAP) in a noncompetitive manner with a $\text{p}K_a$ of 7.1.²¹ However, the binding mode and location of phosphate could not be determined in the previous study.

Phosphate inhibition of native and Co derivatives of sAP intensifies as the pH decreases, showing $\text{p}K_a$ values that are consistent with the ionization constant of H_2PO_4^- reported at 7.12 at 25 °C.²⁹ The smaller values of the dissociation constant K_i at lower pHs indicate that it is preferably the monobasic form H_2PO_4^- rather than the dibasic form HPO_4^{2-} that binds sAP. This can be due to the presence of a carboxylate such as Glu131 in close proximity of the active-site metal ions (Figure 1).¹⁷ The more negative dibasic HPO_4^{2-} formed at higher pH may generate larger electrostatic repulsion with the Glu131 side chain. On the other hand, hydrogen bonding between the negatively charged Glu131 side chain and the OH group of monobasic phosphate would increase phosphate binding affinity, thus enhancing the inhibition at $< \text{pH } 6.0$. The similar $\text{p}K_a$ values for phosphate binding to the different metal-substituted derivatives of sAP indicate that the protonation process of phosphate is not affected by the different Lewis acidities of the metal ions (i.e., the dinuclear ZnZn, CoCo, and CoZn centers). The result also reflects that the phosphate may not bind to the

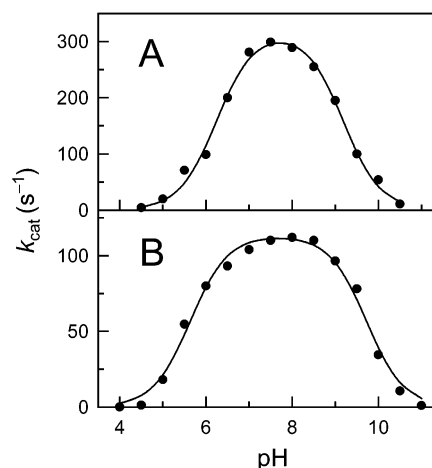


Figure 4. pH-dependence of k_{cat} of (A) ZnZn-sAP and (B) CoCo-sAP in the absence of Ca^{2+} . The data have been fitted to the equation $k = k_{\text{limit}} / (1 + [\text{H}^+]/K_1)(1 + K_2/[\text{H}^+])$ for a two-proton ionization process to yield $k_{\text{limit}} = 320 \pm 20 \text{ s}^{-1}$, $\text{p}K_1 = 6.30 \pm 0.07$, and $\text{p}K_2 = 9.20 \pm 0.06$ for ZnZn-sAP and $k_{\text{limit}} = 113 \pm 8 \text{ s}^{-1}$, $\text{p}K_1 = 5.50 \pm 0.05$, and $\text{p}K_2 = 9.70 \pm 0.05$ for CoCo-sAP.

metal ions that are directly involved in substrate binding in crystallographic studies of several APs,^{8–17} which is consistent with the observed noncompetitive inhibition kinetics wherein phosphate does not compete with the substrate in binding to the active site.

The phosphate inhibition constants K_i vary significantly for ZnZn-, CoZn-, and CoCo-sAP at pH 6.0 (0.80, 8.2, and 9.1 mM, respectively). This observation indicates that the binding of phosphate to the enzyme is affected by the different metal ions in the active site, whereas the deprotonation process of phosphate is not. Thus, deprotonation of phosphate must occur prior to its binding to the enzyme. The results also imply that the “first” metal binding site in sAP has a strong influence on phosphate binding to sAP since CoZn-sAP and CoCo-sAP with a Co^{2+} ion in their “first” site have similar K_i values; whereas ZnZn-sAP with Zn^{2+} in the “first” site shows a significantly different K_i value. The difference is possibly due to an electrostatic repulsion between the phosphate inhibitor and the attacking nucleophile, which is a coordinated hydroxide in a metal-centered hydrolysis.³⁰ A metal center of stronger Lewis acidity should generate a higher mole fraction of the coordinated hydroxide nucleophile than a weaker Lewis acidic metal under the same conditions, thus a higher K_i value for phosphate inhibition due to a larger electrostatic repulsion. This hypothesis can be further investigated in pH-dependent activity studies discussed below.

The pH–activity profiles of the first-order rate constant (k_{cat}) for ZnZn-sAP and CoCo-sAP display a typical bell-shaped curve which can be fitted to a two-proton ionization process (Figure 4) to afford the ionization constants of the general base and the general acid in the ES complex.^{28,31,32} ZnZn- and CoCo-sAP are found to have different first ionization constants ($\text{p}K_{\text{es1}} = 6.3$ and 5.5, respectively). The

(28) Cornish-Bowden, A. *Fundamentals of Enzyme Kinetics*, rev. ed.; Portland: London, 1995.

(29) Meites, L. *Handbook of Analytical Chemistry*; McGraw-Hill: New York, 1963.

(30) Kimura, E.; Koike, T. *Adv. Inorg. Chem.* **1997**, *44*, 229–261.

(31) Cleland, W. W. *Methods Enzymol.* **1982**, *87*, 390–405.

(32) Tipton, K. F.; Dixon, H. B. F. *Methods Enzymol.* **1979**, *63*, 183–234.

activation of the enzyme associated with pK_{es1} must be due to the deprotonation of the nucleophilic metal-bound water in the active site of sAP, which is close to those of the metal-bound water in carboxypeptidase A³³ and thermolysin.³⁴ Moreover, fluoride inhibition of ZnZn-sAP revealed a pK_{a} of 6.2, which was proposed to be associated with a metal-bound water.²¹ Since the pH profile of the second-order rate constant $k_{\text{cat}}/K_{\text{m}}$ is controlled by the pK_{a} values of both the free enzyme and the free substrate (such as the amino group of Leu-*p*NA with a pK_{a} of 7.74³⁵), it cannot afford specific information about the ionization status of the coordinated water and thus is not discussed further here.

At pH 8.0 ($>pK_{\text{es1}}$), phosphate inhibition displays similar K_{i} s of ~ 40 mM for the Co²⁺-substituted derivatives (insets, Figure 3) and 31 mM for native sAP,²¹ whereas the K_{i} values for the Co²⁺-substituted sAP derivatives and native sAP²¹ differ by about 10-fold at pH 6.0 ($\sim pK_{\text{a}}$). The discrepancy of the K_{i} values of phosphate between native sAP and its Co²⁺ derivatives can result from different magnitude of the electrostatic repulsion between phosphate and the metal-bound OH⁻. The local concentration of OH⁻ is approximately 6-fold higher in CoCo-sAP than in native sAP at pH 6.0 (i.e., [OH⁻]/[H₂O] ratio of the coordinated water is 3.2 in CoCo-sAP with pK_{a} of 5.5, whereas it is only 0.5 in native sAP with pK_{a} of 6.3). The higher mole fraction of metal bound OH⁻ in the ES complex of CoCo-sAP can weaken phosphate binding to a much higher degree than in the case of native sAP at pH 6.0 but not at pH 8.0. The inhibition constant K_{i} in a pure noncompetitive inhibition can represent the binding of the inhibitor to either the enzyme or the ES complex to give EI or the ESI ternary complex.²⁸ Thus, results for phosphate binding to the ES complex described above are also applicable to phosphate binding to the free enzyme E.

Chemical Modification of Arginine. Phosphate and phosphate moiety have been shown to bind to positively charged residues such as arginine and lysine.³⁶ Since the crystal structure of sAP illustrates that there is an arginine residue near the active site (Arg202, which, however, is not completely revealed in the crystal structures),^{16,17} arginine modification with phenylglyoxal was performed and the modified enzyme was further investigated. Phenylglyoxal reacts with the guanidinium group on arginine via the Schiff-base condensation reaction,²⁵ thus placing steric hindrance on the side chain of arginine without altering its positive charge. The modified arginine side chain is stable under acidic conditions and dissociates to regenerate arginine on prolonged incubation under neutral and alkaline conditions.³⁶

Table 1. Rate Constants and Phosphate Inhibition Constants of ZnZn-sAP (A), CoCo-sAP (B), and CoZn-sAP (C) and Their Phenylglyoxal-Modified Derivatives for Leu-*p*NA Hydrolysis at pH 6.0

	k_{cat} (s ⁻¹)	K_{m} (mM)	K_{i} (mM)
A ^a	425 ± 23	2.2 ± 0.1	0.75 ± 0.06
modified A ^a	70 ± 4	19 ± 2	7.7 ± 0.4
B	83 ± 6	1.6 ± 0.2	7.9 ± 1.2
modified B	42 ± 3	6.6 ± 0.6	76 ± 10
C	90 ± 5	4.3 ± 0.1	8.2 ± 0.3

^a In the presence of 10 mM CaCl₂, except for K_{i} determinations using the Dixon plot.

The modification of sAP is complete in a few hours with a pseudo-first-order rate constant of $2.1 \pm 0.3 \text{ h}^{-1}$ based on the rate in decreasing activity. The modification of ZnZn- and CoCo-sAP with phenylglyoxal results in a significant change in the kinetic parameters K_{i} , K_{m} , and k_{cat} for the hydrolysis of Leu-*p*NA (Table 1). The inhibition constants K_{i} s are 10-fold higher for both derivatives after the modification, suggesting that arginine is involved in phosphate binding. The Michaelis constant (K_{m}) is also significantly changed, displaying an 8-fold increase for ZnZn-sAP and a 4-fold increase for CoCo-sAP. The rate constant k_{cat} is lowered by $\sim 85\%$ for ZnZn-sAP and $\sim 50\%$ for CoCo-sAP after the modification (Table 1). These significant changes in kinetic parameters reflect that arginine is involved in the catalytic action of this enzyme. Modification beyond 4 h shows little changes in the kinetic parameters. The condensation reaction is reversible,³⁶ which allows the activities of ZnZn-sAP and CoCo-sAP to recover to full extents after prolonged incubation of the modified enzyme at pH 8.5 and 4 °C, as verified with their kinetic parameters.

Modification of sAP with phenylglyoxal is not specific for any of the 8 arginine residues in sAP. However, if an arginine is involved in phosphate binding, incubation of the enzyme with phosphate prior to modification should protect it from the modification to a certain extent. In addition, since the transition-state analogue 1-aminobutylphosphonate is a strong inhibitor of sAP toward peptide hydrolysis,³⁷ it should protect an Arg from modification to a certain degree if the Arg is involved in binding of the inhibitor and in stabilizing the transition state of peptide substrates. The protection experiments were accomplished by incubating the enzyme in the presence of an inhibitor with a concentration greater than $10K_{\text{i}}$ of the inhibitor prior to and during modification. The modification reactions in the presence of the “protection agents” were stopped after 30 min of incubation to make certain that the reactions have not reached completion in order to reveal any discrimination against modification due to inhibitor binding.

The results reveal that the enzyme samples modified in the presence of phosphate or 1-aminobutylphosphonate exhibit significantly higher activity than the samples modified without any inhibitor (Table 2), indicating that the modification is inhibited by the inhibitors. The protection against the modification by the transition-state analogue 1-aminobutyl

(33) Kunugi, S.; Hirohara, H.; Ise, N. *Eur. J. Biochem.* **1982**, *124*, 157–163.

(34) Makinen, M. W.; Wells, G. B.; Kang S.-O. *Adv. Inorg. Biochem.* **1984**, *6*, 1–70.

(35) Baker, J. O.; Prescott, J. M. *Biochemistry* **1983**, *22*, 5322–5331.

(36) (a) Riordan, J. F. *Mol. Cell. Biochem.* **1979**, *26*, 71–92. (b) Kawase, S.; Cho, S. W.; Rozelle, J.; Stroud, R. M.; Finer-Moore, J.; Santi, D. V. *Protein Eng.* **2000**, *13*, 557–563. (c) McGuire, M.; Huang, K.; Kapadia, G.; Herzberg, O.; Dunaway-Mariano, D. *Biochemistry* **1998**, *37*, 13463–13474. (d) Gutknecht, R.; Lanz, R.; Erni, B. *J. Biol. Chem.* **1998**, *273*, 12234–12238.

(37) (a) Park, H. I.; Ming, L.-J. *Angew. Chem., Int. Ed.* **1999**, *38*, 2914–2916; *Angew. Chem.* **1999**, *111*, 3097–3100. (b) Park, H. I. Ph.D. Dissertation, University of South Florida, Tampa, FL, 1999.

Table 2. Rate Constants and Phosphate Inhibition Constant of ZnZn-sAP in the Presence and Absence of Inhibitors during Modification by Phenylglyoxal^a

inhibitor	k_{cat} (s ⁻¹)	K_{m} (mM)	$k_{\text{cat}}/K_{\text{m}}$ (s ⁻¹ mM ⁻¹)	K_{i} (mM)
none	234 ± 2	0.69 ± 0.06	340	51 ± 1
phosphate	285 ± 2	0.37 ± 0.02	770	38 ± 1
αBP ^b	272 ± 1	0.47 ± 0.01	580	43 ± 1

^a The modification is terminated before completion (after 30 min), and then the inhibitor was removed. The assays were performed in the presence of 10 mM CaCl₂ at pH 8.0. The K_{i} values were determined without Ca²⁺ at pH 8.0, which results in the relatively larger inhibition constants. ^b 1-Aminobutyl phosphonate.

phosphate (which bind to the active site of the enzyme) reflects that the modified arginine(s) must be in very close proximity of the active site, which leaves Arg202 as the most probable candidate (cf. Figure 1). The modification of Arg202 and its involvement in phosphate binding is further corroborated by the observation that the analogous AP from *Aeromonas*, which does not have an Arg residue close to the active site^{14,15} as Arg202 in sAP, is not inhibited by phosphate at basic and neutral pHs and is only very weakly inhibited ($K_{\text{i}} \sim 100$ mM) by phosphate in a *competitive manner* at pH 6.0.

³¹P NMR for Phosphate Binding. The binding of phosphate to the paramagnetic CoCo- and CoZn-sAP to form the corresponding EI complexes can be monitored by the enhancement in ³¹P NMR relaxation rates of phosphate at pH 6.5. Since the inhibition constant K_{i} in a pure noncompetitive inhibition represents inhibitor binding to both the ES and the ESI complexes,²⁸ the binding information obtained in the NMR study is thus comparable to the kinetic results about phosphate binding to the ES complex described above.

There is no ³¹P NMR signal observed when the samples were initially analyzed, verifying that phosphate does not accumulate during purification process. The paramagnetic contribution toward ³¹P NMR relaxation rate ($T_{1\text{p}}^{-1}$) of phosphate was obtained by subtracting the relaxation rate of phosphate in the presence of the diamagnetic ZnZn-sAP (161 s⁻¹) from the measured T_1^{-1} value in the presence of a paramagnetic Co²⁺-substituted sAP under the same conditions. Significant $T_{1\text{p}}^{-1}$ values were obtained which indicates that the increase in relaxation rate is due to the interaction of phosphate with the paramagnetic Co²⁺ center in the active site of sAP.

A plot of ³¹P NMR relaxivity (i.e., the normalized relaxation rate $T_{1\text{p}}^{-1}/[\text{E}]$, with [E] being the concentration of a paramagnetic Co²⁺ derivative) versus phosphate concentration in the presence of each of the Co²⁺ derivatives is shown in Figure 5. Much larger $T_{2\text{p}}^{-1}$ values (over 100 times) than $T_{1\text{p}}^{-1}$ values are observed at every phosphate concentration (data not shown), indicating that $T_{2\text{p}}^{-1}$, but not $T_{1\text{p}}^{-1}$, is determined predominantly by the chemical exchange between free and bound phosphate.³⁸ The relaxivity as a function of phosphate concentration can be fitted to the following

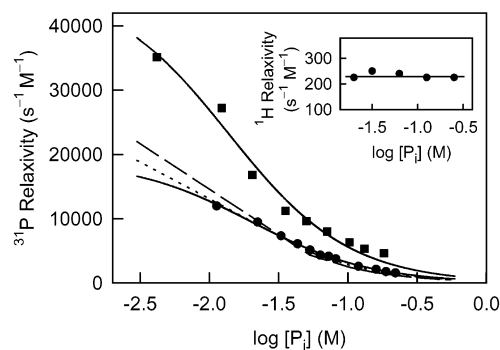


Figure 5. Dependence of ³¹P NMR relaxivity $T_{1\text{p}}^{-1}/[\text{E}]$ of phosphate at 145.73 MHz in the presence of CoZn-sAP (●) and CoCo-sAP (■) at pH 6.0. The solid traces are the best fits of the data to eq 2. The dotted trace represents the ³¹P NMR relaxivity of CoCo-sAP divided by 2, and the dashed trace represents the difference between the relaxivities of CoCo-sAP and CoZn-sAP. The inset shows the relaxivity of the ¹H NMR signal at 360.13 MHz of the bulk water as a function of phosphate concentration. The enzyme concentrations were 1–2 mM, and the phosphate concentrations varied from 10 to 250 mM.

equation for a single phosphate binding site to afford the relaxation rate of the bound phosphate, $T_{1\text{M}}^{-1}$.^{26,27,38}

$$T_{1\text{p}}^{-1}/[\text{E}] = T_{1\text{M}}^{-1}K_{\text{f}}/(1 + K_{\text{f}}[\text{P}_{\text{i}}]) \quad (1)$$

Here K_{f} is the affinity constant for phosphate binding. The K_{f} values of 50.1 and 72.7 M⁻¹ and $T_{1\text{M}}^{-1}$ values of 381 and 639 s⁻¹ are obtained for CoZn- (●, Figure 5) and CoCo-sAP (■, Figure 5), respectively, from the fittings (solid traces, Figure 5). The K_{f} values for the formation of the enzyme–phosphate EI complexes can be converted to dissociation constants (20.0 mM for CoZn-sAP and 13.8 mM for CoCo-sAP), which are close to the K_{i} values obtained from kinetic inhibition measurements at pH 6.5 for the two derivatives (14.1 and 17.0 mM, respectively, Figure 3 insets).

The $T_{1\text{M}}^{-1}$ value obtained from eq 1 can be related to the Co²⁺–³¹P distance, r , according to the Solomon equation³⁹ by assuming a predominant dipolar contribution to the relaxation (eq 2), where C is a group of physical constants and $f(\tau_{\text{c}})$ is the correlation function. The metal binding sites of sAP are better described to be five-coordinate on the basis of the electronic spectra of the Co²⁺ derivatives of the enzyme in solution.²² With application of the lower limit of the electron relaxation time of 10⁻¹² s for high-spin Co²⁺ in a five-coordinate environment,²⁶ the minimum ³¹P–Co²⁺ distance is obtained to be 4.1 Å in phosphate-bound CoZn-sAP according to eq 2. This distance is much larger than expected for a phosphate directly coordinated to a metal center, which would give P–metal distances of ~2.9 Å in sAP on the basis of the crystal structure of the enzyme with a “bound phosphate”.¹⁶ Moreover, the through-bond delocalization of unpaired electrons from a paramagnetic metal center onto a coordinated phosphate can afford significant contact relaxation of the ³¹P signal which would result in an underestimated metal–P distance of about 2.5 Å or less as previously observed in the case of direct phosphate binding

(38) Mota de Freitas, D.; Luchinat, C.; Banci, L.; Bertini, I. Valentine, J. *S. Inorg. Chem.* **1987**, *26*, 2788–2791.

(39) Solomon, I. *Phys. Rev.* **1955**, *99*, 559–564.

to the metal center in the Co^{2+} -substituted derivatives of superoxide dismutase.^{40,41}

$$T_{\text{IM}}^{-1} = Cr^{-6}f(\tau_c) \quad (2)$$

Since eq 1 is valid for a single paramagnetic center, a value for the ^{31}P - Co^{2+} distance in CoCo-sAP can only be estimated with an assumption that the magnetic coupling between the two Co^{2+} ions is weak and the two paramagnetic centers contribute to the relaxation independently.^{26,27} Accordingly, an averaged relaxation contribution from one Co^{2+} center in CoCo-sAP can be estimated by dividing phosphate relaxivity by 2 and then fitted with eq 1. The fitting affords a T_{IM}^{-1} of 319 s^{-1} , which gives a ^{31}P - Co^{2+} distance of 4.2 \AA (dotted trace, Figure 5). This longer distance than that in CoZn-sAP can be due to (a) the presence of magnetic coupling is not taken into account or (b) the bound phosphate is farther away from the second metal site. Magnetic coupling between the two site is present in the case of CuCu-sAP.²² If this is also the case in CoCo-sAP, then the distance is overestimated. Thus, an upper limit of the Co^{2+} - ^{31}P distance can be estimated by subtracting the relaxivity in CoZn-sAP from that of CoCo-sAP and fitted to eq 1, affording a T_{IM}^{-1} value of 270 s^{-1} , which corresponds to a ^{31}P - Co^{2+} distance of 4.3 \AA (dashed trace, Figure 5). The results conclude that phosphate cannot be bound directly to the metal ions in the active site of sAP in solution. Instead, phosphate is located 4.1 – 4.3 \AA away from the metal center and bind to a positively charged group near the active site, likely Arg202.

The inset in Figure 5 illustrates that the ^1H NMR relaxation of the bulk water signal of CoCo-sAP solution remains unchanged at different phosphate concentrations ($230 \pm 10 \text{ s}^{-1} \text{ M}^{-1}$). If phosphate were to bind to the metal center of the enzyme in solution as proposed in the crystal structure,¹⁶ it would replace one or more coordinated water molecules. In this case, a noticeable or significant change would be expected in the ^1H NMR relaxation of the bulk water signal when the coordinated water molecules are exchangeable with the bulk water, which is expected since Co^{2+} ion is highly labile.⁴² This observation rationalizes the noncompetitive phosphate inhibition kinetics, corroborating that phosphate is not bound to the dimetal center of sAP.

Insight into the Mechanism of sAP. The results presented here indicate that the phosphate binding site in sAP is Arg202, which is also involved in binding with transition-state inhibitors such as 1-aminobutylphosphonate. Thus, Arg202 must play an important role in the stabilization of the transition state during sAP catalysis. Moreover, the weakly competitive inhibition manner of phosphate at pH 6.0 toward the analogous AP from *Aeromonas* lacking an Arg near the active further implies the significance of Arg202 in sAP for phosphate binding. A simple molecular modeling finds that low-energy conformers of Arg202 can be created

with the guanidinium group located near the metal ions (Figure 1). A phosphate bound to one of the Arg202 conformers (stick-and-ball presentation, Figure 1) would give a metal- ^{31}P distance around 4.0 – 4.5 \AA . The lack of a hydrophobic moiety in phosphate seems to prevent it from binding to the active-site metal ions. On the other hand, in the case of the inhibition by 1-aminoalkylphosphonates and *p*-nitrophenyl phosphate,³⁷ the inhibitors may be anchored into the active site by hydrophobic recognition which thus results in a competitive inhibition pattern. Moreover, rotation of the C–C bonds of Arg202 side chain can create another conformer (thin-line presentation, Figure 1), which can bring the guanidinium group within H-bonding distance to the *gem*-diolate moiety of the transition state, supporting the involvement of Arg202 in the action of sAP and the binding of transition-state analogues.

In combination with previous studies of sAP and other dinuclear APs,^{12,14,17,21} the results reported here have lead to the following mechanism for sAP catalysis of peptide hydrolysis. First, the N-terminal amino group of the peptide substrate binds to one of the Zn^{2+} ions, while the carbonyl oxygen is stabilized by the other or both Zn^{2+} ions. The nucleophilic water is formed at this stage, which then attacks the carbonyl carbon to form the *gem*-diolate transition state. The transition state can be further stabilized by Arg202 through hydrogen bonding. The role of Arg202 in sAP action is thus similar to the role of Arg127 in the action of carboxypeptidase A⁴³ in stabilizing the tetrahedral *gem*-diolate transition state.

Recently, sAP has been revealed to exhibit a unique “alternative catalysis”, in which the transition state-like phosphodiester bis(*p*-nitrophenyl) phosphate and the phosphonate ester *p*-nitrophenyl phenylphosphonate are effectively hydrolyzed by sAP and its several metal-substituted derivatives with catalytic proficiencies (k_{cat}/k_1) reaching 10 billion and 0.3 million, respectively.^{37,44} It is of great interest to point out that an Arg side chain has been shown in crystallographic studies to be involved in the catalytic action of several metallophosphoesterases and phosphotransferases.⁴⁵ Our finding here about the role of Arg202 of sAP in phosphate binding and in stabilizing the transition state in peptide hydrolysis suggests that this residue may also be important in rendering the unique alternative catalysis of sAP possible. Verification of this hypothesis awaits future investigation of mutants by means of kinetic methods.

Acknowledgment. The authors thank Altan Ercan for providing the data about phosphate inhibition of *Aeromonas* AP. The support of this study by the Petroleum Research Fund, administered by the American Chemical Society (Grant ACS-PRF #35313-AC3), is acknowledged.

IC025584F

(40) Banci, L.; Bertini, I.; Luchinat, C.; Monnanni, R.; Scozzafava, A. *Inorg. Chem.* **1987**, *26*, 153–156.

(41) Ming, L.-J.; Valentine, J. S. *J. Am. Chem. Soc.* **1990**, *112*, 4256–4264.

(42) Cotton, F. A.; Wilkinson, G. *Advanced Inorganic Chemistry*, 5th ed.; Wiley: New York, 1988; Chapter 29.

(43) Christianson, D. W.; Lipscomb, W. N. *Acc. Chem. Res.* **1989**, *22*, 62–69.

(44) Ercan, A.; Park, H. I.; Ming, L.-J. *Chem. Commun.* **2000**, 2501–2502.

(45) Lipscomb, W. N.; Strater, N. *Chem. Rev.* **1996**, *96*, 2375–2433.